J Comp Physiol A (2002) 188: 753–766
DOI 10.1007/s00359-002-0362-2

ORIGINAL PAPER

W. D. Chapple

Mechanoreceptors innervating soft cuticle in the abdomen of the hermit crab, *Pagurus pollicarus*

Received: 28 May 2002 / Revised: 15 August 2002 / Accepted: 14 September 2002 / Published online: 26 October 2002

Abstract Mechanoreceptors in the soft cuticle of the 4th abdominal segment of the hermit crab, *Pagurus pollicarus*, that are associated with reflex activation of abdominal postural motoneuron, were studied to determine whether their properties are consistent with a feedback control of abdominal stiffness. Three classes of receptors were identified: (1) setal dome receptors, (2) hypodermal receptors, and (3) funnel-canal receptors. The hypodermal receptors, which have the largest extracellular action potentials, were selected for further study. Their axons innervate the entire ipsilateral half of a segment; receptive fields of receptors with different amplitudes show extensive overlap. They are phasic and show significant adaptation; at higher frequencies they signal displacement rather than velocity. Although they are activated by changing muscle tension, their threshold for cuticular displacement is much lower than for forces generated by postural muscles. These features suggest that they are primarily involved in signaling cuticular displacement and shearing forces as they contact the columella of the shell in which the hermit crab lives.

Keywords Crustacea · Hermit crab · Hypodermal receptor · Mechanoreceptor · *Pagurus*

Abbreviations *DSM* dorsal superficial muscles · *PSDF* probability spike-density function · *PSTH* peristimulus time histogram · *VSM* ventral superficial muscles

Introduction

Research in the last 20 years has fundamentally altered our view of how mechanoreceptors participate in the control of posture and locomotion. For many years, it was believed that this control was executed by negative feedback, but it is now recognized that proprioceptors play a more complex role (Horak and MacPherson 1996). During different phases of the locomotor cycle, for example, tendon organs may augment or inhibit muscle tone (Pearson and Collins 1993); muscle spindles may signal muscle length and velocity, or extreme joint angle to trigger the transition between extension and flexion (Hiebert et al. 1996). These different actions appear to rule out simple linear control models that might regulate stiffness or muscle length. This state dependency of mechanoreceptor input appears to be a general feature of motor systems since it is also found in arthropod motor system (DiCaprio and Clarac 1983).

Although proprioceptors play the major role in mechanoreceptor control of movement, other mechanoreceptors can participate in and modulate central nervous system pathways generating movement (Duysens et al. 2000). In arthropods, many receptors on the cuticle are activated by muscle activation or cuticular strains generated by movements (Zill and Moran 1981; Libersat et al. 1987). Moreover, internal mechanoreceptors, regarded as proprioceptors, may be activated by external mechanical stimuli, such as sound (Pflüger and Field 1999). Thus, there may be no close correspondence between receptor type and its role in a specific movement. A further difficulty is that, in many animals, mechanical coupling between different tissues makes it difficult to determine how precisely a receptor is tuned to variables important in motor control. This difficulty is particularly acute in mechanoreceptors associated with soft tissues since stresses that activate receptors may be generated at considerable distances from the receptor and are then filtered by the visco-elastic properties of the tissues.

It is therefore particularly interesting to examine the mechanoreceptors controlling movement in an arthropod in which there is an ill-defined distinction between receptors associated with a flexible cuticle and those associated with internal tissues such as muscles and connective tissue. The hermit crab abdomen, homologous to

W.D. Chapple
Department of Physiology and Neurobiology,
University of Connecticut, Storrs, CT 06269-4156, USA
E-mail: chapple@predator.pnb.uconn.edu
Tel.: +1-860-4864558
Fax: +1-860-4863303

the calcified abdomens of macrurans, has become soft and decalcified as an adaptation for supporting the gastropod shell in which hermit crabs live. The superficial abdominal muscles are primarily used to increase the tone of the abdominal hydrostatic skeletal system (Chapple 1993) and support the shell. The ventral superficial muscles (VSM) have several layers of longitudinal muscle fibers, as in macrurans, but superficial to them are additional layers of muscle fibers oriented in a circular and transverse orientation. In the mid-abdominal segments, the fast extensor muscles and the muscle receptor organs of macrurans have been lost, so that there is only a single layer of longitudinal muscle fibers beneath the dorsal abdominal surface, the dorsal superficial muscles (DSM). All of these muscles are coactivated by mechanoreceptors associated with the cuticular region of the mid-abdomen. Previous studies identified one class of phasic receptors that did not appear to be associated with any specialization of the cuticle (Chapple 1966; Bent and Chapple 1977). These receptors could be activated by superficial muscle activity, increasing muscle tone by positive feedback (Chapple 1993), as well as touch. This reflex saturates and adapts, resulting in a regulation of abdominal stiffness (Chapple 1997). This role of positive feedback to control posture requires further examination since it has been recognized for many years that positive feedback can produce destructive instabilities. An alternative hypothesis is that the biologically relevant stimulus is external displacement of the cuticle as it rubs against the shell; muscle activation of the receptors might be incidental to this stimulus.

The results will show that the sensory receptors are more diverse than was originally believed; there are at least two, possibly three classes of receptors associated with soft cuticle, hypodermal receptors, setal domes, and funnel-canal organs, and that at least two of them activate the motoneurons. The hypodermal receptors respond to both touch and muscle force, but are more sensitive to touch. They are activated by low velocities of cuticular displacement, but at higher velocities they are more sensitive to the amplitude of displacement than to velocity. They exhibit a pronounced adaptation of their response. Those receptors with the lowest thresholds are not associated with the major mass of the VSM but with the lateral portions of the segmental circumference that contacts the columella of the shell in which the hermit crab lives. Thus, instead of acting as part of a local feedback loop regulating muscle force, these receptors are better situated to detect changing contact between the columella of the gastropod shell and the lateral surface of the abdomen.

Materials and methods

Pagurus pollicarus were collected from sublittoral protected areas in Fishers Island Sound off the coast of Connecticut. Two preparations using the isolated abdomen (separated from the thorax at the thoracic-abdominal junction) were used to study the mechanoreceptors: (1) a dissected preparation, and (2) an 'intact' preparation. In both preparations, a thermoelectric cooler maintained the abdomen at 12.5°C. in Cole's solution.

Dissected preparation

In the dissected preparation, the posterior abdomen was exposed with a longitudinal incision along its medial dorsal surface, the hepatopancreas removed, and the abdominal nervous system was exposed by removing the large fast flexor muscles of the 3rd, 4th and 5th segments (Chapple 1997). The first roots of the 4th abdominal ganglion were exposed laterally by removing the overlying longitudinal muscle fibers of the 3rd segment. Most experiments were performed on the right 1st root since this is composed almost entirely of sensory afferents.

Intact preparation

In the 'intact' preparation, the isolated abdomen was unopened and the hepatopancreas was left in place, so that cuticular stresses were similar to the normal animal. The abdomen was mounted ventral side up, and a small slit made in the cuticle above the 4th abdominal ganglion to expose the 1st roots. This did not obviously alter the shape of the abdomen, since the hepatopancreas is located in the dorsal part of the abdominal cavity and is prevented from moving out of the ventral slit by the attachments of the deep flexors to the ventral body wall. The right 1st root was cut proximal to the ganglion and drawn into a suction electrode.

Potentials from nerves were recorded either with glass suction electrodes or by using bipolar platinum hook electrodes with a nerve drawn into paraffin oil. Signals were amplified with an A-M Systems differential a.c. amplifier with a passband of 10 Hz to 1 kHz and digitized at 5 kHz with a Data Translation DT3831 I/O board mounted in a computer. EMG recordings from VSM muscles were made by implanting a 75-μm Teflon-coated silver wire between the superficial and deep muscle layers; the indifferent electrode was placed within the hepatopancreas. Since the amplitude of extracellular signals varied between preparations, amplitudes were expressed in multiples of the discrete voltage levels of the A/D converter rather than in microvolts (100 $\mu V = 1650$), because an amplitude class has quite different absolute voltage ranges in different preparations. The convention for identifying nerves was described in Chapple (1997). Briefly, the abdominal segment is specified, followed by the side, and the number of the ganglionic root; thus, 4r1 is the right first root of the 4th ganglion.

A number of different stimulus devices were used to excite the mechanoreceptors: (1) a handheld probe mounted on a force transducer, (2) the same probe mounted on a solenoid, and (3) the same probe mounted on a servo-controlled loudspeaker. Both the solenoid device and the servo-controlled stimulator were controlled by a custom computer program. The solenoid received a gating pulse that turned it on or off; a fine tungsten wire on the tip of the solenoid probe delivered a constant step increase in force to the skin surface. Although this device delivered constant force steps, the oscillations at the onset and offset of the stimulus made it less useful for studying receptor dynamics. The servo-controlled system was composed of a loudspeaker, the amplitude of movement of which was measured with a linear diode (UDT LSC/5D, UDT Sensors, Hawthorne, Calif., USA) excited by an infrared LED mounted on the cone of the loudspeaker. The length signal was sent to a PID controller and then to a power operational amplifier (Burr-Brown 3573AM) connected to the loudspeaker. Ramp signals were generated by the computer; in some experiments, a Wavetek 188 Sweep/Function Generator was gated by the computer to produce sinusoids of different frequencies.

Digitized records of extracellular spike trains were displayed offline in Matlab (The MathWorks, Natick, Mass., USA). A threshold was set visually so that the amplitudes (maximum positive excursion plus the maximum negative excursion) and spike

times (cross-over point from a positive to negative potential) for all spikes above that threshold were recorded in a table. An amplitude histogram of all the spikes for that channel in an experimental file (typically ten trials) was constructed and the lower and upper boundaries for a desired amplitude class selected. These selected spikes were then displayed superimposed in contrasting colors over the original record to confirm that the desired spike class was correctly selected and that it was composed of a discrete group of spikes. In favorable recordings, this procedure reliably isolated a spike amplitude class that was assumed to reflect the activity of a single unit. However, stimuli to different portions of the cuticle evoked similar amplitudes of action potentials and it could not be assumed that they represented the same unit. Thus, it was not possible to reliably map the receptive field of a single amplitude class. Moreover, during a burst of action potentials evoked by high rates of cuticular strain, the extracellular record was often too complex to permit spike discrimination by this method; under these conditions, data from a trial was not included in further calculations. Action potential frequencies are described as pulses per second (pps) to distinguish them from stimulus frequencies (Hz).

To calculate the average response of a unit to repeated presentations of a stimulus, a probability spike-density function (PSDF) was calculated. In contrast to the peristimulus time histogram (PSTH), it provides a continuous rather than a discrete estimate of the probability of firing (Silverman 1986; Richmond et al. 1987) and circumvents the error in the estimate of the probability of spike occurrence near bin edges. It was calculated by convolving the time of each spike with a Gaussian distribution kernel with a fixed standard deviation five times the sampling frequency for the output array. The PSDF was then normalized by dividing by the integral of the kernel. Means and standard errors of the estimate (SEE) of a series of trials were calculated and their values at particular times used to estimate significant differences between experimental procedures. The PSDF acts as a low-pass filter, with units expressed in probabilities from 0 to 1. A standard deviation (SD) of 5 ms (probability/1 ms) resulted in a cutoff frequency (–3 dB) of 17.4 Hz and a standard deviation of 50 ms resulted in a cutoff frequency of 1.46 Hz.

First roots that were to be examined with a light microscopy were either fixed in Bouin's fixative, embedded in paraffin, cut at 10 μm, and stained with Mallory's trichrome or Heidenhain iron hemoxtoxylin (Presnell and Schreibman 1997). Some samples that were epoxy embedded for transmission EM (TEM) were also sectioned and stained for light microscopy (LM).

Samples for LM, TEM and scanning electron microscopy (SEM) were fixed in modified Karnovsky fixative (glutaraldehyde 1.5%, formaldehyde 1.5%, cacodylate buffer 0.15 mol l^{-1}, pH 7.4, $MgCl_2$ 3 mmol l^{-1}, sucrose 20%), and then post-fixed in 2% osmium tetroxide in cacodylate buffer. For LM and TEM, samples were dehydrated in a graded ethanol series followed by propylene oxide, and then embedded in epoxy resin. Sections of 1–2 μm were cut and stained in toluidine blue for LM, while sections of 100 nm were cut and stained with lead citrate and uranyl acetate for TEM. For SEM, samples were dehydrated in a graded ethanol series, then critical-point dried and sputter-coated with gold-palladium. TEM was carried out on a Philips EM300 at 80 kV. Negatives were digitized at 600 dpi. SEM was carried out on a LEO 982 FESEM.

Results

External morphology of the posterior abdomen

When a hermit crab is supporting its shell during quiet standing, its abdomen is rotated to the right about the thoracic-abdominal junction (Fig. 1A). The last three segments are further twisted to the right by the ventral superficial muscles. The telson and uropods are thus rotated 90°, so that the right uropod extends above and the larger left uropod below the abdomen to contact the lumen of the shell and anchor the end of the abdomen within it. Because of this rotation, the region of the posterior abdominal surface that bears the weight of the shell and contacts it during movement is not the ventral midline of the abdomen but a region 30–40° from the ventral midline to the right.

The cuticle of the posterior abdomen is quite complex. Each dorsal portion of a segment is composed of a rostral and a caudal region (Fig. 1B), both of which are separated from the ventral region by the lateral groove, a longitudinal band of amuscular cuticle that separates the lateral margin of the VSM from the DSM. At the rostral margin of each segment, there is a partially calcified pleuron, on which, on the left side, pleopods and their musculature are located while on the right side only the faint outlines of the less calcified pleuron can be observed. The pleura of each side merge with the tergum to extend from the lateral groove around the dorsal circumference of the abdomen. Between the pleura-tergum regions of each segment, there is a caudal region of soft uncalcified cuticle, the articular membrane, overlying the DSM that extend caudally in a single layer to the margin of the next segment (Chapple 1977a). The DSM originate on the caudal margin of one pleuron and insert on the rostral margin of the pleuron of the next segment. In contrast to the DSM, the VSM are continuous along the longitudinal axis, with only the intersegmental tendons that attach the deep abdominal muscles to the cuticle to indicate the transition from one segment to another.

Each segment is also divided around its circumference into different regions that extend longitudinally the length of the segment. For a distance of about 3 mm on either side of the ventral midline, the abdominal surface is unpigmented and smooth. At the lateral margins of this zone groups of red and yellow chromatophores appear, arranged in transverse lines 0.2–0.4 mm apart. The surface becomes uneven, composed of peaks and crevasses in the cuticle 0.2–0.3 mm in extent. In addition, there are domes of cuticle (Fig. 1C) about 0.2 mm apart with five or six setae 200–300 μm long (Fig. 1D), arranged in longitudinally aligned rows. These rows of domes extend laterally to the region of the lateral groove and a millimeter or so dorsal to it. Dorsal to the lateral groove the cuticular surface becomes smoother; red, blue, and gold chromatophores are numerous and extend to the dorsal midline. The setal domes are not only found on the right side; the domes and their setae are actually more prominent on the left side, facing the lumen of the shell, where they are larger and with longer setae than on the right side, particularly on the ventral third segment just caudal to the columella protuberance. In addition to setal domes, clusters of very small (diameters of about 3 μm) structures (Fig. 1E) with hemispherical shapes and a complex folded center are also present in different areas of the abdominal surface, resembling funnel-canal organs described in other decapods (Gnatzy et al. 1984; Shelton and Laverack 1968).

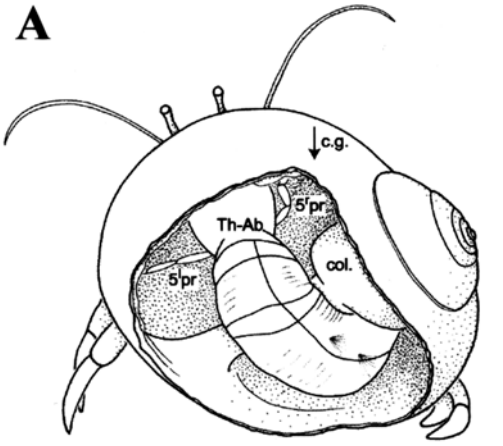

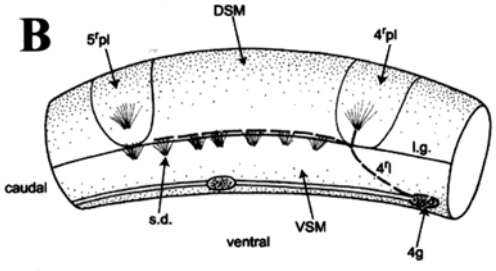

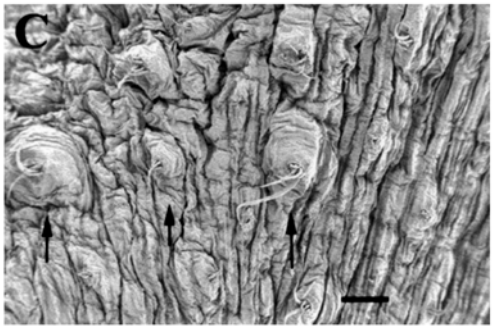

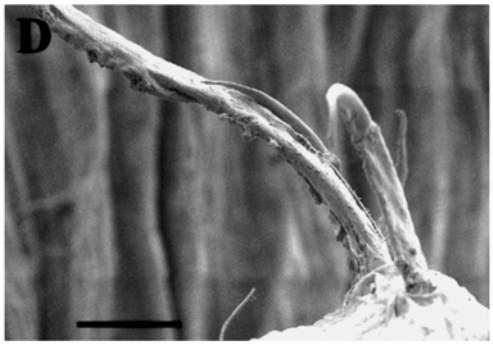

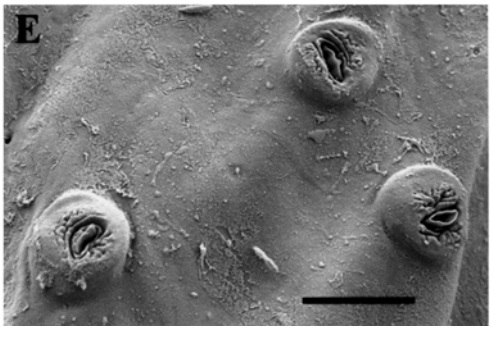

◀

Fig. 1A–E Morphology of the abdomen and its cuticle. **A** Rear view of *Pagurus* in its shell. *col.* columella of the shell, *c.g.* shell center of gravity, *Th-Ab.* thoracic-abdominal junction, *5^{r}pr.* fifth right walking leg, *5^{l}pr.* fifth left walking leg. **B** Diagram of 4th segment, right parasagittal view. *DSM* dorsal superficial muscles *l.g.* lateral groove, *VSM* ventral superficial muscles, *s.d.* row of setal domes, *4 g.* 4th ganglion, *4^{r}1.* right 1st root, 4th ganglion, *4^{r}pl.* fourth right pleuron, *5^{r}pl.* fifth right pleuron. **C** Scanning electron microscopy (SEM) of several rows of setal domes (*arrows* indicate individual domes of one row). Calibration bar: 200 μm. **D** SEM view of a setal dome. Calibration bar: 50 μm. **E** SEM of putative funnel-canal organ. Calibration bar: 5 μm

Morphology of afferent nerves

Mechanoreceptor afferents are found in all three of the ganglionic roots. The 1st roots of the 4th ganglion contain a large number of afferents and, on the left side, the axons of motoneurons to the pleopod muscles (Bent and Chapple 1977). The 2nd roots contain mechanoreceptors that innervate the ipsilateral pleuron (Chapple 1977b). In 3rd roots, in contrast to lobster and crayfish, there are afferents as well as motor fibers. The 1st ganglionic roots of each abdominal ganglion appear to contain the majority of afferents entering the ganglion. The 1st roots of the 4th abdominal ganglion, used in these experiments, run peripherally from the caudal ventral surface of the ganglion, entering the VSM at the abdominal ventral midline superficial to the ganglion. They run laterally and superficially in a narrow channel between the VSM and the cuticle to the ventral caudal margin of the partially calcified pleuron where they send branches to different regions of the pleuron, a distance from the ganglion in large animals of over 15 mm. One branch innervates sensory setae on the pleuron, as well as pleopod muscles on the left side (Bent and Chapple 1977). A large branch runs caudally along the lateral groove sending fine nerves out to innervate both ventral and dorsal regions of the soft cuticle of the segment. It is possible to expose the 1st roots along their path to the pleuron; fine processes can be seen to exit at points along their path. Methylene blue staining of the right 1st root of the 4th ganglion revealed a diffuse arrangement of bipolar cells close to the point at which the 1st root branches at the ventral margin of the right pleuron. These cells (Fig. 2A, B) are often clustered together so that in fixed material, a transverse section may contain a number of cell bodies (Fig. 2B); these cells are approximately 40 μm in diameter with lengths of

▶

Fig. 2A–E Histology of right 1st root, 4th ganglion. **A** longitudinal 2-μm section of a group of bipolar cells (*arrows*). **B** Transverse 2-μm section of four bipolar cells (*arrows*). **C** Transmission electron microscopy (TEM) section of a bipolar cell with prominent nucleus and nucleolus. The nucleus is surrounded by an inner zone of rough endoplasmic reticulum (ER), a middle zone of smooth ER and Golgi apparatus, and an outer lightly stained rind possibly containing cytoskeletal elements. Calibration bar: 5 μm. **D** TEM section of the middle zone of a bipolar cell showing two Golgi complexes. Calibration bar: 1 μm. **E** TEM section of a portion of the 1st root, showing larger axons enclosed in glial sheaths and bundles of smaller axons contained within a common sheath. Calibration bar: 1 μm

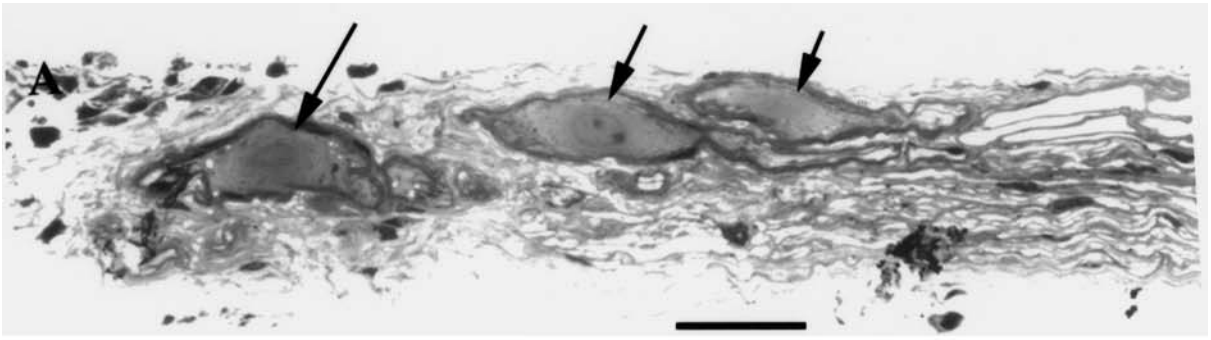
A

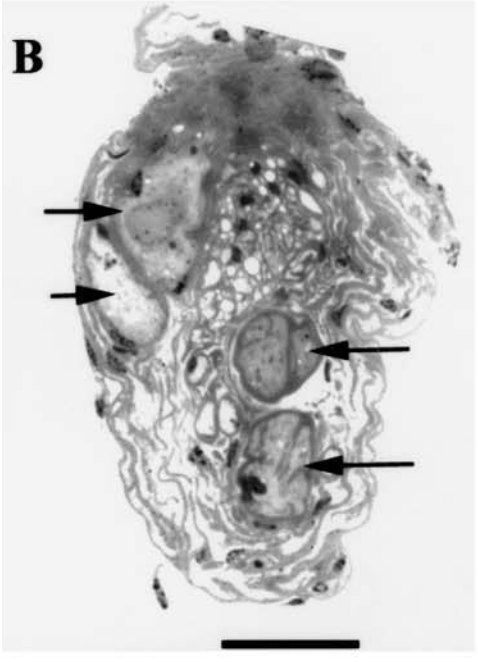
B

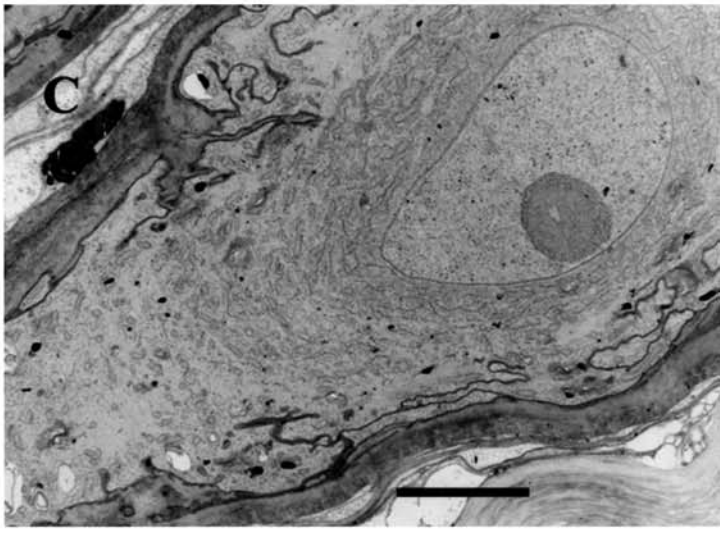
C

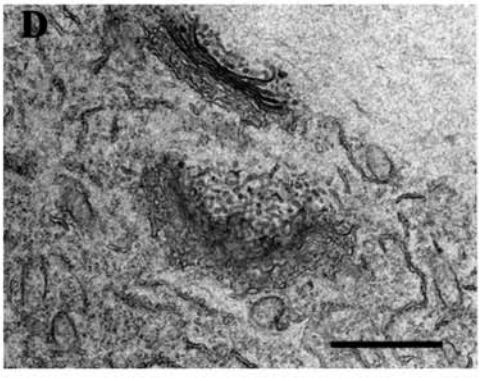
D

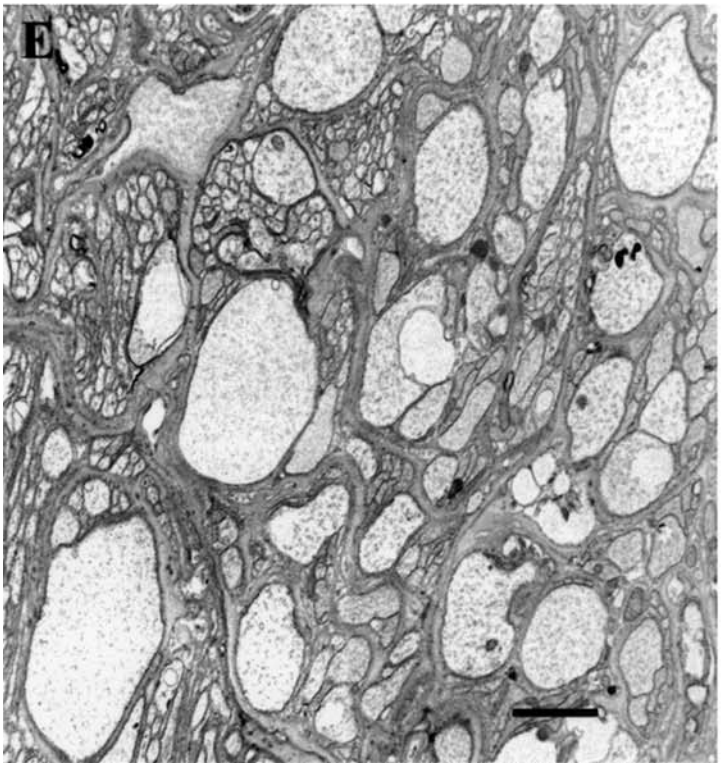
E

about 120 μm. An EM section of one of these cells (Fig. 2C) shows a prominent nucleus with a single nucleolus. A region of rough endoplasmic reticulum and ribosomes surrounds the nucleus, and surrounding it is a region of smooth endoplasmic reticulum and numerous Golgi complexes (Fig. 2D). Adjacent to the surface of the cell is a clear region that may be composed of cytoskeletal elements. A dense glial sheath surrounds the plasma membrane of the cell. In transverse sections of the 1st root, there are numerous axons as well, some with diameters of 2–3 μm surrounded by ensheathing glia as well as populations of much smaller axons with diameters in the range 0.1–0.2 μm enclosed in the same ensheathing glia (Fig. 2E).

Receptor diversity

Three classes of mechanoreceptors were identified, two of which were examined electrophysiologically.

The first class of mechanoreceptors is not associated with external features of the cuticle and is assumed to consist of hypodermal receptors (Bush and Laverack 1982). These receptors have been previously described in hermit crab (Chapple 1966; Bent and Chapple 1977) and crayfish (Pabst and Kennedy 1967). They respond to touch to the cuticle (Fig. 3A) with thresholds in the order of 0.5 mN, to jets of saline projected onto the cuticular surface, and during activation of the underlying muscles (Chapple 1993). In crayfish, Pabst and Kennedy (1967) identified the large somas of bipolar cells that were activated by touch to the cuticle; these were located within the first roots close to the ganglion, but were not associated with superficial structures of the soft cuticle. Thus, it is likely that the bipolar cells found in the distal portion of the first roots in hermit crab may be the cell bodies of homologous receptors. However, as a result of the extensive investment of connective tissue around the somas of these cells it has not been possible to record intracellularly from them.

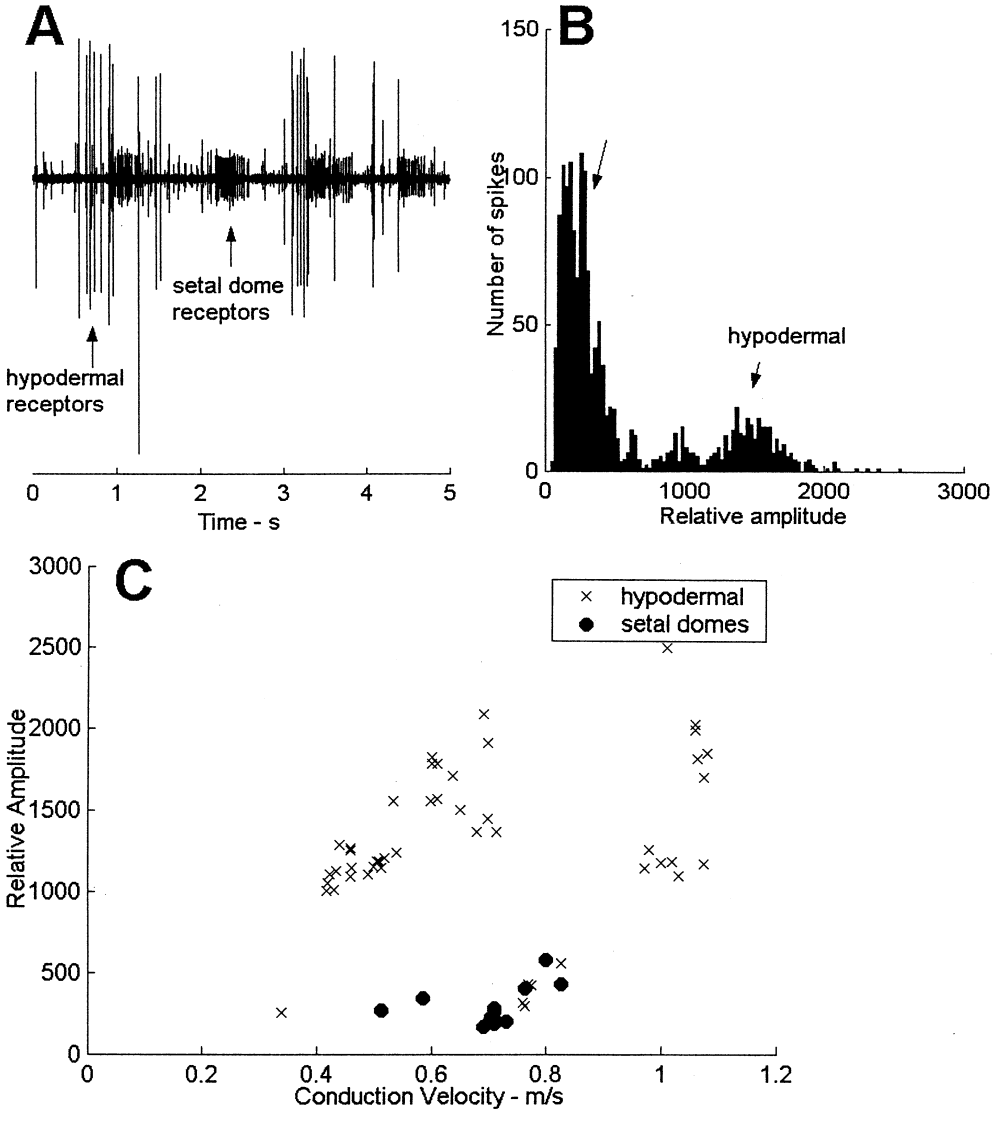

Fig. 3A–C Extracellular properties of two classes of mechanoreceptors in the right 1st root of the 4th ganglion. **A** Activation of the larger amplitude spikes of hypodermal receptors by light touch, and smaller amplitude spikes of setal dome receptors by deflection of the setae. **B** Extracellular amplitude histogram of action potentials in 4r1 over ten trials showing the differences in the amplitudes of the two receptor classes. **C** A plot of relative extracellular amplitude (recorded at the distal branch point of 4r1) versus conduction velocity for 71 spikes shows that amplitude and conduction velocities of the two classes are not linearly related. Conduction velocities measured between the distal branch point of 4r1 and proximal entrance to the 4th ganglion, hook electrodes in paraffin oil

A fine probe was initially used to activate these receptors. Extracellular action potentials recorded from the branch of the 1st root running caudally along the lateral groove were correlated with action potentials recorded at the entrance of the 1st root into the 4th ganglion. This suggests that the majority of these afferents have distal processes that support action potentials. Very light touch or displacement of the cuticle did not activate these receptors; the cuticle must be depressed enough to press against the underlying pigmented layer that lies between muscle fibers and the cuticle itself. Shear of the cuticle above a sensitive region of the hypodermis did not reveal any difference in threshold for activating a receptor as the direction of shear was changed. Careful removal of the cuticle superficial to the hypodermal layer did not abolish receptor response, indicating that their activation did not depend upon the integrity of the cuticle or cuticular structures.

A second class of mechanoreceptor potentials is associated with setal domes (Fig. 3A). These receptors had extracellular amplitudes that were much smaller than those of hypodermal receptors. Their potentials were only detected when the 1st root was placed on a hook electrode and surrounded with paraffin oil instead of recording with a suction electrode. Amplitude histograms of 1st root mechanoreceptor spikes (Fig. 3B) showed that peaks associated with setal dome receptors have 10–20% of the amplitudes of typical hypodermal receptors. Sustained deflection of the setae on the dome to an angle of greater than about 50° in either direction normal to the plane of the row of setae produces a burst of action potentials with peak frequencies of 50 Hz, lasting for about 400 ms (Fig. 3A).

To discriminate between the two classes of receptors using other criteria than amplitude, a second criterion of axon size, conduction velocity, was measured by recording from the right 1st root of the 4th ganglion at two different points on the nerve with hook electrodes. A plot of the extracellular amplitudes of receptors, recorded at the distal electrode, as a function of conduction velocity showed that this was not a linear relationship (Fig. 3C), but contained several discrete clusters. Potentials associated with setal domes had conduction velocities centered around 0.75 m s^{-1}, similar to conduction velocities of hypodermal receptors with much greater extracellular amplitudes obtained from the same experimental trial. Moreover, extracellular amplitudes at the two recording sites, particularly those in the group of largest extracellular potentials, were often quite different.

Area of 1st root innervation

Since many 1st root mechanoreceptors reflexly activate VSM motoneurons, the region of a segment innervated by them is important in assessing their role in motor control. For example, a region restricted to the cuticle overlying the VSM might suggest local regulation of tone. A more extensive area might suggest a relatively non-specific feedforward activation of motoneurons by external stimuli. In a series of nineteen preparations, the 1st roots of the 4th ganglion were drawn into a suction electrode to explore the receptive fields of hypodermal receptors; initially a tungsten needle probe was used to explore the surface of the 4th segment, pinned out as a flat sheet. The region innervated by the 1st root included both the dorsal and ventral portions of the ipsilateral segment, roughly extending from the dorsal to ventral midline. Longitudinally, the receptive fields of 1st root afferents extended from the rostral edge of the 4th pleuron to the rostral margin of the 5th. The threshold of units located ventrally appeared to be higher than at the lateral groove and the dorsal surface of the hemi segment. Motoneurons of the VSM were activated by mechanoreceptors located in both the dorsal and ventral regions of the segment.

Since it appeared that receptors located on the ventral surface of the abdomen had higher thresholds and lower frequencies than receptors in the area of the lateral groove and the dorsal surface, a quantitative estimate of these differences was performed. In two experiments, the probe was placed at different locations on the cuticle, using a square reticule mounted in the dissecting scope to record position. The probe with a von Frey hair mounted on a solenoid producing a constant step force of 5 mN, was placed at each location and all of the sensory action potentials elicited in a 5-s trial were counted; ten trials were obtained at each point. Figure 4A shows the average number of spikes per trial at different locations over the 4th right segment in one experiment. The mean number of spikes was significantly different in the shaded dorsolateral region (region 7 through 11 compared with 1 through 6, t-test, $P < 0.05$). This experiment sampled sites over the entire segment so that most areas were not sampled. In Fig. 4B, a strip of the abdominal surface extending from the ventromedial to the shaded dorsolateral portion of the segment just caudal to the 4th right pleuron was mapped. Spike number per trial increased monotonically ($P < 0.001$, 14 sites) as the probe was moved laterally.

It was not possible to estimate the receptive fields of individual units. At threshold, several amplitude classes were present in the extracellular record. When a fine suction electrode was placed against the skin to activate units electrically, several classes of action potentials were also observed at threshold. In addition, units with the same extracellular amplitudes could be activated by pressure at different discontinuous points in an area. As displacement amplitude increased, more units were evoked, either because of differences in threshold of units directly beneath the probe or because the mechanical stimulation of the skin displaced regions further from the stimulus site as the stimulus increased in intensity. It was possible to make a transverse cut along the caudal margin of the fourth right pleuron to reduce the number of receptors. In this case, responses from units with similar amplitudes could be elicited from

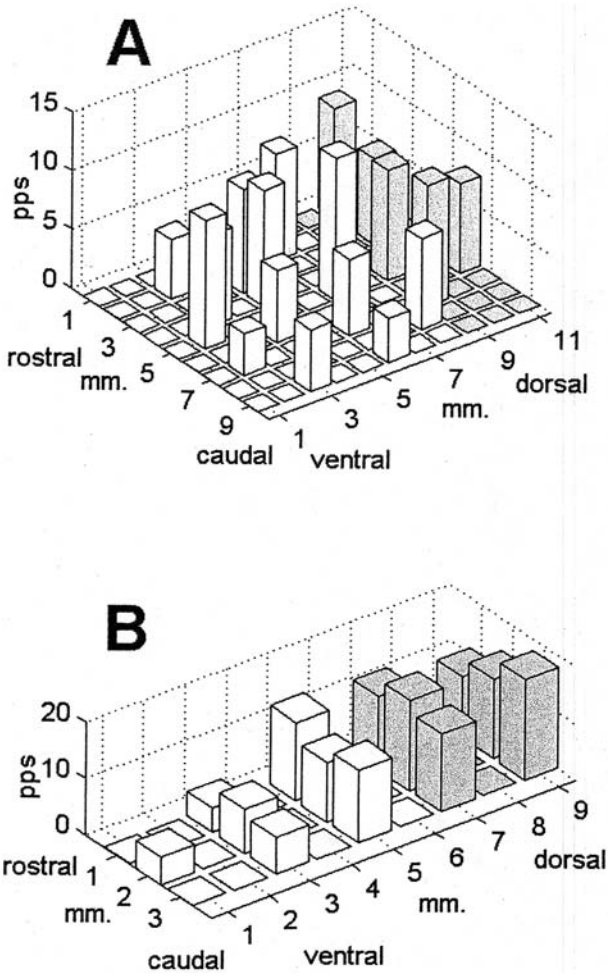

Fig. 4A,B Innervation fields of 1st root mechanoreceptors, 4th ganglion for two preparations. Receptors located dorsal to the lateral groove are activated at higher frequencies to the same amplitude stimulus. The average number of spikes per trials (spk/trial) during ten 5-s trials is plotted as a function of position on the right 4th segment (*shaded bars* indicate the lateral groove and dorsal cuticle). A step displacement of the cuticle was applied with a von Frey hair mounted on a solenoid. **A** Preparation in which the entire right half of the segment was mapped. **B** Preparation in which a narrow strip caudal to the right pleuron was mapped

a 25-mm^2 region. However, such a unit might have a larger field that was disrupted by the cut.

Hypodermal receptor modality

Hypodermal receptors can be activated by a variety of mechanical stimuli, but it was not clear what their normal mode of activation is. In an earlier series of experiments (Chapple 1993) isometric activation of the VSM produced a burst of large action potentials in 4r1, suggesting that these receptors signaled muscle force. In those experiments, the DSM had been removed and there may have been some movement of the cuticle in the region of the lateral groove, so that it seemed important to investigate receptor modality further.

In seven experiments, the VSM was mounted with two plastic plates glued transversely to the surface of the cuticle so that the ventral regions of the DSM as well as the lateral groove were stabilized. As in the earlier experiments, the motor nerve, 4r3, was placed on a stimulating electrode and the activity of 4r1 was recorded with a suction electrode. A stimulus train at 60 Hz evoked an isometric contraction of the muscle. A light touch normal to the cuticular surface (Fig. 5A) evoked a vigorous discharge of afferents; in contrast, isometric tetanus produced a weak low-frequency train of stimuli. It is difficult to specify the difference in force levels activating the receptors by the two routes since the component of force produced by the probe parallel to the surface (which would be recorded by the force transducer) would be small; a touch of 0.5 mN to the cuticle produced a burst of action potentials, an isometric contraction of 120 mN produced a weak increase in tonic firing of the receptors. Because touch to the skin produces a more rapid rate of strain of the cuticle than does activation of the underlying muscle, it is possible that some of the difference in threshold between muscle activation and touch is due to the different stimulus velocities. Figure 5B, a plot of the averaged PSDF for ten trials, shows that during isometric contraction the selected sensory fiber fired at an average rate of 10 pps throughout the duration of isometric contraction with isometric force reaching a peak of 120 mN. Towards the end of two of these experiments, the attachment of the cuticle along one edge of the plate loosened, permitting local movement of the skin, resulting in a more vigorous activation of the receptors when the muscle was activated. This suggests that relative movement rather than average longitudinal stress of the cuticle resulting from muscle activation is the effective stimulus for the receptors.

A complication in assessing the threshold of mechanoreceptors to muscle activation is that, in the intact preparation, the abdomen is a hydrostat in which abdominal muscles contract against hemolymph and hepatopancreas to maintain abdominal tone. By removing the hepatopancreas and laying the abdomen out as a flat sheet, the coupling between mechanoreceptors and muscles is substantially altered. In two animals, it proved possible to cut a small slit in the cuticle above the right 1st root of the 4th ganglion and record from sensory afferents in a situation in which the shape and internal pressure of the abdomen were similar to intact animals. In Fig. 5C, after cutting 4r1 proximal to the recording electrode, the left 5th segment cuticle, which is not innervated by 4r1, was lightly touched. This elicited a vigorous reflex activation (dotted line) of the VSM (as well as deep fast muscles) followed by an activation of the mechanoreceptor receptors that occurred about 120 ms after the beginning of reflex activation of the muscles, indicating that in the intact abdomen, muscle activation in the physiological range can activate the hypodermal mechanoreceptors. However, 2 s into the trial, the sensory response had returned to control levels, although

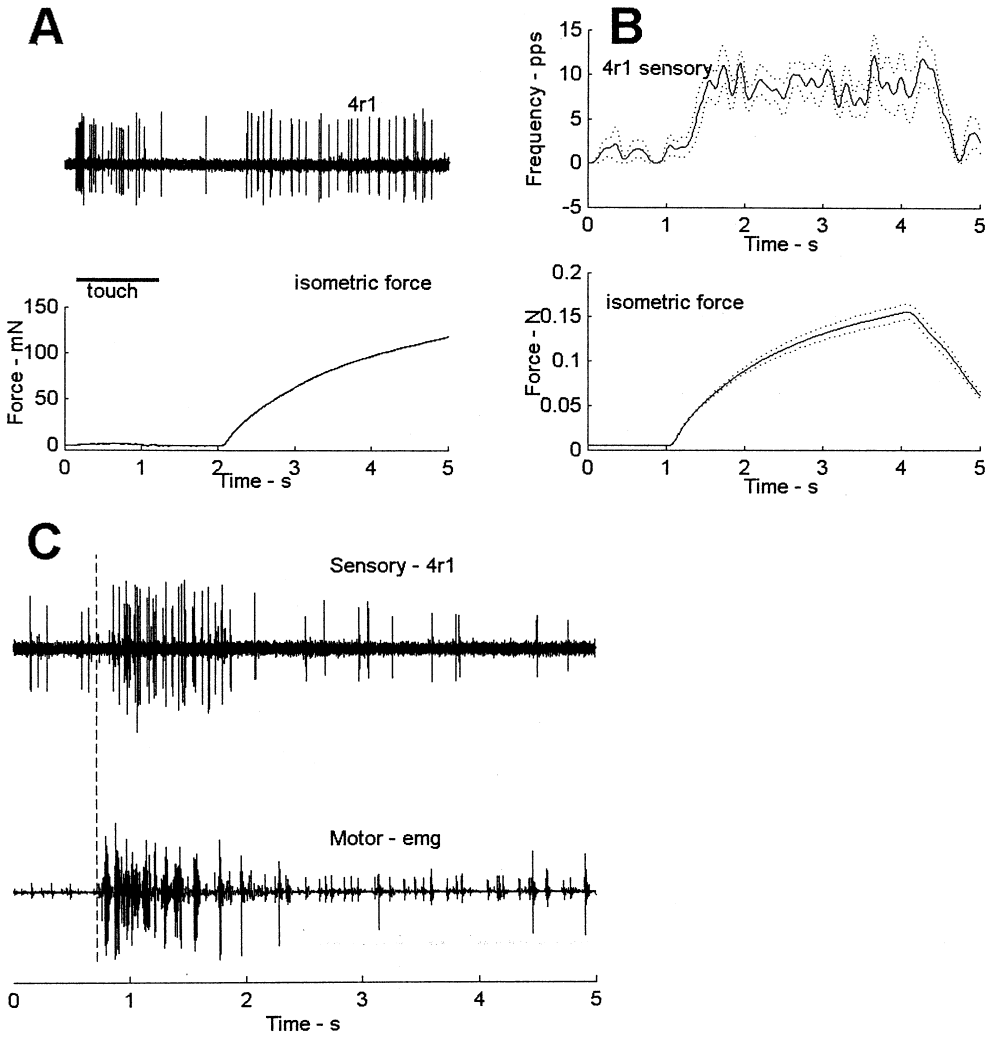

Fig. 5A–C Hypodermal receptor activation by touch and isometric muscle activation. **A** Light touch to the cuticle evokes a high-frequency burst of receptor action potentials (*left*); isometric muscle stimulation activates the receptors weakly (*right*), suggesting that these receptors are primarily activated by contact forces on the cuticle. **B** Probability spike-density function (PSDF) average of ten trials (*dots*, SEE). Isometric activation of the muscle weakly activates the sensory receptor for the entire duration of the stimulus train. **C** 'Normal pressure' preparation, touch to 5th segment left lateral cuticle evokes a reflex activation of VSM muscles (*dotted line* shows beginning of EMG burst), followed by activation of 1st root mechanoreceptors. *Gray bar* beneath the right portion of the record shows VSM tonic elevated firing that does not result in activation of hypodermal receptors, suggesting that even in the intact abdomen the receptors are relatively insensitive to changes in muscle tension

the EMG record showed that motor activity of VSM units (gray horizontal bar) is elevated over control levels (as can be seen in the first 0.5 s of the trial). This is consistent with the observations in the isolated abdomen that the hypodermal receptors are less sensitive to cuticular stresses generated by muscle activation than to normal force on the surface of the cuticle.

Dynamic response

To study the frequency response of hypodermal mechanoreceptors, receptors were activated by displacing the cuticle with a servo-controlled probe directed normal to the cuticular surface (Fig. 6A). At the end of each experiment, a histogram of action potential amplitudes was constructed; under favorable recording conditions, a limited number of discrete amplitudes were recorded. Each discrete amplitude peak could be fit with a Gaussian probability distribution; their standard deviations were not significantly different from one another (Fig. 6B), suggesting that each peak was produced by a single receptor. In addition, a light touch with a fine probe to a specific site on the cuticle produced a burst of potentials of similar amplitudes at about 50 Hz, reinforcing the assumption that each amplitude peak was generated by a single receptor.

Figure 6A shows a representative trial in which a probe displaced the cuticle with a constant velocity, maintained a constant position and then returned to its initial position at the same velocity. There was a burst of action potentials from several amplitude classes at the beginning of stretch. A second burst was associated with the retraction of the probe from the cuticle. Within the burst at the beginning of stretch, two amplitudes, s200 and s600, were selected for further analysis (Fig. 6A, bottom trace); spike classes that were not selected are drawn with a dotted line, while the selected amplitude class is drawn with a solid line. After a variable latency from the onset of stretch, there was a burst of potentials at 40–50 Hz. At the end of the ramp, the frequency of the units dropped rapidly to control levels during the constant length portion of the probe displacement. An examination of the period of the burst, using averaged PSDFs for ten trials (Fig. 6C), showed that at higher ramp velocities the frequency was relatively constant

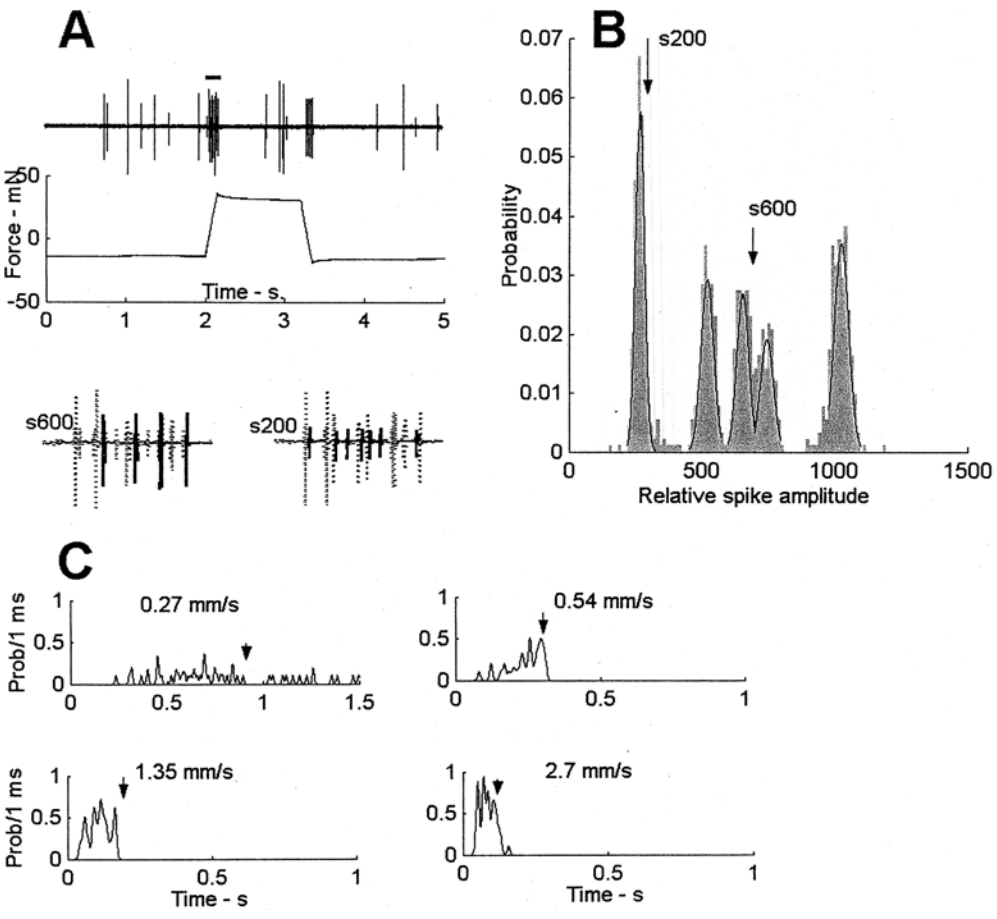

Fig. 6A–C Illustration of the method of isolating and studying a selected amplitude class of hypodermal receptors. **A** *Top trace* shows afferent activation by ramp displacement of the cuticle, followed by a hold period, and a ramp release. *Bar* above the extracellular trace shows the portion of the record expanded in the bottom trace to show the isolation of two receptor classes (*dark lines*), one with a mean of 600 and the other with a mean of 200. Spikes not selected are drawn in *dotted lines*. *Middle trace* shows the force record of the ramp displacement. **B** Amplitude histogram (10 trials) of the extracellular spikes of which **A** is one trial. Gaussian probability distributions were calculated from the means and standard deviations of each of the five amplitude classes and superimposed on the histogram. *Arrows* point to the two classes selected in a. **C** Averaged (ten trials) PSDF of four ramp displacement at different velocities. *Arrows* point to the end of ramp stretch. The absence of peaks at the beginning and end of stretch is consistent with a receptor that signals velocity, not acceleration

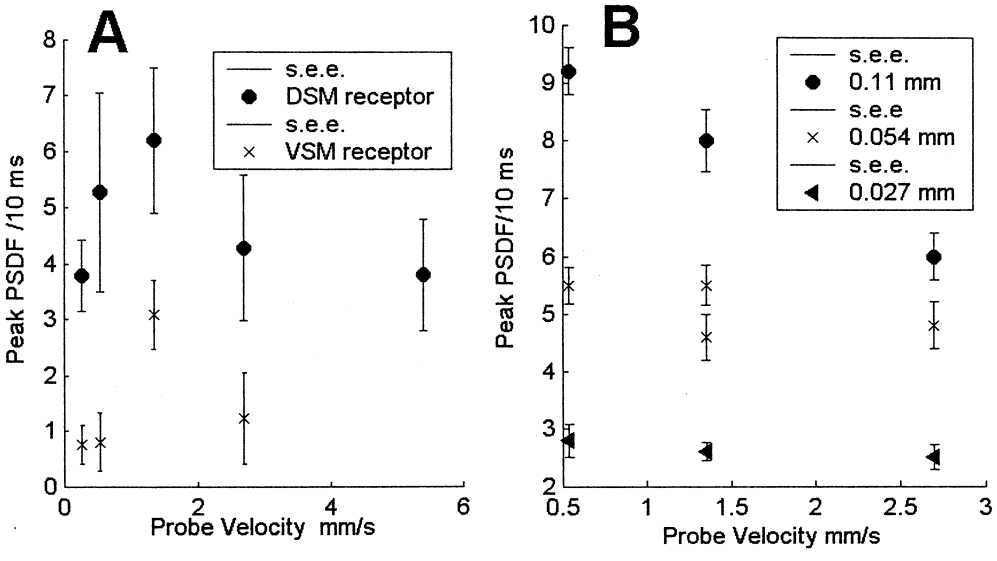

Fig. 7A,B Hypodermal receptor response to ramp cuticle displacement of different velocities and amplitudes. **A** Peak PSDF versus velocity for two units, one (*open circles*) located in the DSM cuticular region, and one (*crosses*) in the VSM cuticular region. Both receptors reach a peak response below 1 mm s^{-1} and their response then decreases at higher stretch velocities. **B** Peak PSDF versus velocity for one unit at three different displacements, showing that above a threshold velocity the receptors behave as displacement receptors

throughout the ramp and then decreased, consistent with the hypothesis that the receptors signaled velocity. In five experiments examined in detail, there was no indication that a receptor fired at the beginning of ramp stretch became silent during its constant velocity period, and fired a second time at the beginning of the holding period at the new length, indicating that the response of the receptors did not contain substantial acceleration components.

Figure 7A shows the results, in two receptors from different regions of cuticle, of the velocity dependence of burst frequency. When the rate of stretch was varied and its amplitude remained constant, there was an increase in burst frequency from threshold velocities of

about 0.27 mm s^{-1} to about 1.35 mm s^{-1}. Above this, there was a decrease in frequency, so that velocities of 2.7 mm s^{-1} produced an average probability of firing, for ten trials, that was lower than for ramps of 1.35 mm s^{-1} velocities (Fig. 7A). It is difficult, using a ramp displacement of the cuticle, to measure receptor dynamics over an extended range of probe displacements in this preparation. Under these experimental conditions, in which the amplitude of displacement was held constant, the duration of stimulation will be inversely proportional to the velocity. If the time-constant of the mechanoreceptor is long, relative to ramp duration, this increase in ramp velocity will produce a constant peak response in a linear system. Attempting to circumvent this by using longer ramp durations requires large amplitudes of displacement that deform larger areas of skin and recruit more mechanoreceptors, making interpretation of the extracellular record difficult. In Fig. 7B a similar experiment with a single receptor illustrates that, in addition to velocity, burst frequency was proportional to ramp amplitude.

A second approach to characterizing the dynamics of the receptors was to apply a constant sinusoidal displacement to the cuticular surface (Fig. 8A). At the beginning of the stimulus, the burst correlated with each cycle was composed of a number of spikes from a single amplitude class but as the stimulus continued, fewer and fewer action potentials were evoked. Figure 8B is a plot of the average number of spikes per cycle as a function of increasing cycle time for ten trials. The lower the sinusoidal frequency, the greater the number of spikes that was evoked during the first cycle (since the duration of maximum displacement was greater at lower frequencies). As the number of cycles increased, there was a rapid decrease in the number of spikes with a steady state of one or fewer spikes per cycle reached after five to ten cycles. At higher frequencies, there were frequent failures of spikes generated during a cycle, although, when a spike was generated, it was phase-locked to the stimulus. Receptors did not reliably follow stimulus frequencies above 50 Hz.

To examine the relationship between sinusoidal frequency and the spike times relative to the peak

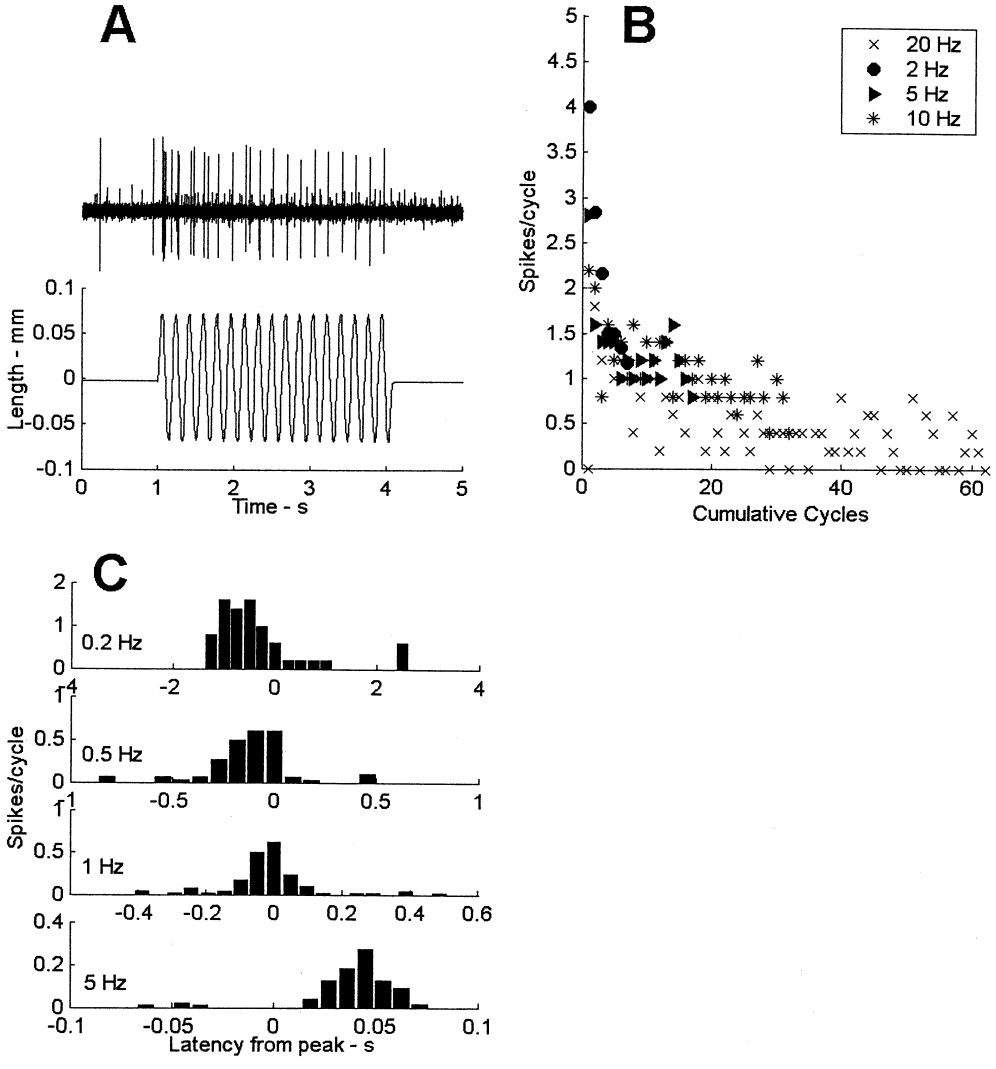

Fig. 8A–C Hypodermal receptor response to sinusoidal cuticle displacement. **A** A 5-Hz stimulus showing an initial burst at the beginning of stimulation, followed by adaptation of the response. After the initial period the unit fires once in each cycle. **B** Time-course of adaptation at different frequencies, showing that the decrease in spikes/cycle is proportional to the number of cycles, which indicates that the change in the response is not due to mechanical characteristics of the cuticle. **C** Latency histogram at four frequencies, calculated from records such as **A**. The receptor fires at different times relative to the peak displacement of the cuticle. The progressive shift in latency is consistent with a low-pass filter model of low-frequency dynamics. Mean latency at 0.2 Hz:–0.40 + 0.60 s (–29°); at 0.5 Hz: –0.11 + 0.30 s (–14°); at 1 Hz: –0.02 + 0.10 s (+18°); at 5 Hz: 0.05 + 0.04 s (+140°)

displacement, a histogram of spike latency relative to the peak was generated for each frequency. At very low frequencies, the peak of the histogram preceded the peak of the sinewave; at 0.2 Hz (Fig. 8C) it was about –400 ms. The duration of the period of firing was about 1 s. As the sinusoidal frequency was increased there was a shift to the right of the peak, so that at 5 Hz the peak was at about +40 ms. In addition, the period during which the probability of firing was high became progressively shorter. At higher frequencies, several peaks in the histogram were observed. To interpret the peak latency at each frequency the time delays associated with activation of a receptor and its conduction time to the electrode must be measured. A step displacement was used to estimate this time; step displacement (time to peak of 5 ms) activated a burst of action potentials after 30 ms from the step to the first action potential in a burst. Thus, at sinusoidal frequencies above 15 Hz, spikes initiated in the previous cycle would appear as a negative latency peak in the histogram, and, as the frequency was increased, multiple peaks would be observed (as was the case). The latencies of the peaks at higher frequencies is likely to be further influenced, not only by receptor dynamics and the conduction time to the recording site, but by the adaptation mechanisms of the receptor. Thus, peak latencies above 15 Hz were not reliable indicators of receptor dynamics, due to this aliasing, but their presence indicates that the receptors could follow sinusoidal stimuli to 50 Hz. The significance of the peaks was evaluated by assuming that if the spikes were not correlated with the stimulus there would be a uniform distribution of latencies within the histogram. Using 95% confidence limits derived from a uniform random distribution (total number of spikes in 10 trials distributed over 22 bins), all of the peaks in Fig. 8C were significant at the 95% level.

Discussion

Mechanoreceptors of the soft cuticle of the hermit crab abdomen comprise a diverse collection of receptors. In addition to hypodermal receptors, described previously, setal domes and putative funnel-canal organs are present that may activate motoneurons. The entire ipsilateral side of a segment sends information from these receptors via the 1st roots to the ganglion. The hypodermal receptors, which have large spike amplitudes, are activated by light touch on the cuticle as well as active muscle force. They are phasic receptors that respond to very low frequencies of movement but show rapid adaptation of their response, suggesting that they act primarily in a feed forward pathway to increase abdominal stiffness. Although they are activated by increasing muscle force, their thresholds to muscle force are considerably higher than to touch to the cuticle.

Comparison between hermit crab and macruran receptor configuration

The regions of the 4th abdominal segment innervated by 1st root receptors differed between crayfish and hermit crab. In crayfish (Wiersma and Hughes 1961; Wiersma and Bush 1963; Davis 1969) mechanoreceptors in 1st abdominal roots innervate the swimmerets, the ventral margin of the pleuron and the ventral surface of the segment, but the majority of afferents from tergum and lateral areas of the pleuron enter the ganglion via the 2nd roots. In contrast, Bent and Chapple (1977) and the present experiments show that, in *Pagurus*, afferents from the entire ipsilateral portion of the segment enter the ganglion via 1st roots. In addition to innervating the same areas of the segment as in crayfish, there has been an extension of 1st root afferents to regions innervated in crayfish by the 2nd roots. It may be that this is associated with the loss of the deep extensors and the reduction in the size of the superficial dorsal musculature (homologous to the superficial extensors in crayfish) in *Pagurus*, or that it is related to the expansion of areas of the segment containing soft cuticle.

In contrast to the segmental exoskeletal units of tergum and pleural found in macrurans, the soft cuticle of the hermit crab abdomen obscures the segmental boundaries. Nevertheless, the morphology of the abdominal surface is complex. In contrast to the smooth ventral surface that overlies the major mass of the VSM, the more lateral regions of cuticle are corrugated and thrown into folds that may act to increase the friction between shell and abdominal surface. These regions have rows of setal domes, and hypodermal receptors with lower thresholds for touch than ventral regions. As the shell is rotated and depressed during locomotion or displacement by external forces, these receptors would be activated. However, since setal domes and hypodermal receptors are found on the left side of the posterior abdomen as well, they cannot be only specialized for signaling contact with the shell. The left side of the abdomen faces downward towards the floor of the outer lumen of the shell, so these receptors might also signal fluid flow during shell movement. Further examination of the position of the abdomen in the shell will be required to determine the point on the circumference of the abdomen that contacts the shell.

In crayfish (Pabst and Kennedy 1967) and in hermit crab, hypodermal receptor somas are clustered together within the peripheral 1st roots rather than close to the site of transduction, as is the case of many other arthropod mechanoreceptors. In addition, they often have processes that branch to innervate a wide area. Pabst and Kennedy (1967) showed that their receptive fields are broken into sub fields separated by insensitive areas with prominent dendritic knobs at their end-terminals, but it was not possible to examine the receptive fields of individual receptors in hermit crab. Removal of the cuticle does not abolish hypodermal responses in either crayfish or hermit crab. Conduction velocities in both

crayfish and hermit crab were in the range of 0.5–0.8 m s^{-1}. Thus, individual hypodermal receptors appear to be similar in crayfish and hermit crab.

The presence of other types of receptors in the soft cuticle suggests that at least some of the reflex effects observed in motoneurons might be due to setal dome or funnel-canal organ receptors. Unfortunately, setal dome receptors produce small action potentials below the noise level when using conventional suction electrodes, making it difficult to determine whether their actions on motoneurons are different from hypodermal receptors. Further work is also needed to confirm the identity of possible funnel-canal organ receptors on the cuticle. TEM cross-sections of the 1st root show a rich spectrum of large and small fibers, as has been reported from other decapod preparations (Sutherland and Nunnemacher 1968). Many of these may generate action potentials below the noise level for extracellular recordings. Hypodermal receptors could not be reliably differentiated from setal domes based on conduction velocity. This was surprising since the average extracellular amplitude of setal dome action potentials were 15–20% of those of the hypodermal receptors; in theory, conduction velocities should be half of those of hypodermal receptors, instead of being approximately the same. This anomaly could be due to differences in the glial packaging of axons in the nerve that might produce differences in the external resistance surrounding the axons. Thus, although the present experiments deal largely with hypodermal receptors, other classes of receptors are present that can potentially contribute to motoneuron excitation.

Modality of hypodermal receptors

A major question is whether touch or muscle activity is the primary stimulus that excites the hypodermal receptors under normal conditions. In *Pagurus,* light touch (0.5 mN) to the surface produces bursts with spike frequencies of 50–60 pps. Isometric activation of VSM and the subsequent activation of hypodermal receptors under these conditions produced tonic activation frequencies of about 10 pps, at force levels of 150 mN, suggesting that local strains in the tissue beneath the cuticle, not muscle activation, are the relevant stimulus for the mechanoreceptors. Actual thresholds were difficult to measure experimentally since light touch directs a force normal to the cuticular surface, whereas isometric activation produces an axial force that is distributed over an extensive region of the circumference of the VSM. In addition, the rate of displacement of the cuticle during touch is greater than the changes in force during muscle activation.

When the abdomen is left relatively intact and the 1st root isolated peripherally, reflex activation of the muscle surrounding 1st root mechanoreceptors produces an activation of receptors much greater than under isometric "pinned out" conditions. However, based on the amplitude of EMG potentials as well as visual observation of the abdomen, this reflex activation involved deep flexors as well as the VSM. The increased activity of the VSM alone seems to have a much smaller effect on the mechanoreceptors. For this reason, it is likely that during normal postural variations in muscle tone, the mechanoreceptors do not substantially increase their frequency and do not produce a substantial positive feedback action on the motoneurons.

Receptor dynamics

All of the hypodermal receptors were phasic with little response to static levels of force. None of the receptors examined fired only at the beginning and end of a constant velocity ramp, indicating that they were not signaling the acceleration of the probe (a possibility suggested by Chapple 1993). The speed of displacement of the cuticle to which they responded was quite low, often less than 0.2 Hz, the effective limit of the equipment used in these experiments. As the velocity increased, burst frequency increased up to a speed about five times threshold, after which burst frequency did not change with velocity. Using sinusoidal stimuli below 10 Hz, the burst frequency at peak displacement rapidly decreased during the first few cycles to reach a steady-state response of one spike per cycle. At stimulus frequencies of 20 Hz and above receptors either fired intermittently or stopped firing after a second or so. Thus, receptor dynamics is determined by two processes. In the absence of adaptation, the receptors are acting as a high-pass filter at low frequencies with an approximate zero at 0.8 rad s^{-1} and a pole at 1.5 rad s^{-1}. Above this frequency, increases in the rate of firing of the receptor are proportional to probe displacement. The latency of the peak firing of the receptors and its shift with frequency is consistent with this interpretation. At low frequencies, the peak firing occurs before the peak of the sinusoid, but as the frequency increases, there is a progressive shift in latency so that at higher frequencies the peak firing lags the peak of the stimulus. At higher frequencies, the aliasing of the response makes an interpretation of the latencies problematic, but the presence of peaks in the cycle histogram indicates that the stimulus is activating the receptors in a phase locked fashion. The adaptation of the response does not appear to be a function of stimulus frequency, but decreases proportional to cumulative cycle number, suggesting that it is a property of the spiking mechanism of the receptor (Torkkeli and French 2002) rather the viscoelastic properties of the surrounding tissue.

The measurement of the frequency response of hypodermal receptors was complicated by a number of factors, making a plot of receptor dynamics in the form of a Bode plot inadvisable. First, it was not possible, because of the overlap of receptive fields to isolate a single receptor at a range of stimulus amplitudes. Thus, sinusoidal measurements established that receptors were

activated at a specific frequency, but gave no information about the magnitude of the response. Second, due to conduction velocity time delays, measurements above 15 Hz were confounded by aliasing. Third, a Bode plot requires that the system is at least quasi-stationary, but due to the presence of adaptation this requirement could not be satisfied. Thus, only an approximate estimate of one feature of the dynamics, the lower corner frequency, seemed appropriate.

The properties of the hypodermal receptors suggest that they are primarily signaling contact forces on the cuticle. Their activation by changes in muscle force is incidental to their major role in shell support. Moreover, their high-pass filter properties, their adaptation and relatively high threshold to muscle force would make it less likely that they could operate as part of a feedback path to regulate abdominal stiffness. It is possible that the funnel-canal organs might provide tonic cuticular stress information but investigation of the motoneuron responses to VSM stretch do not indicate any tonic component to their activation. Since many mechanoreceptors of soft-bodied invertebrates seem to be primarily phasic (Dorsett 1976), this suggests that proprioceptors require a mechanical system, such as an exo- or endoskeletal system that can distinguish between local and external events. In the hermit crab abdomen, a stable elevation of stiffness may depend more on the properties of muscles than on feedback from mechanoreceptors.

Acknowledgements I would like to thank Jacob Krans and Andrew Moiseff for many insightful discussions and helpful comments on the manuscript, Virge Kaske for the diagrams of Fig. 1A and B, and Marie Cantino, Stephen Daniels, and James Romanow of the University of Connecticut Electron Microscope Facility. I am also very grateful to Mark Grabher and Joseph Healy who provided me with animals. This research was supported by NSF grant IBN-9874499.

References

Bent SA, Chapple WD (1977) Simplification of swimmeret musculature and innervation in the hermit crab, *Pagurus pollicarus*, in comparison to macrurans. J Comp Physiol 118:61–73

Bush BMH, Laverack MS (1982) Mechanoreception. In: Atwood HL, Sandeman DC (eds) The biology of Crustacea. Academic Press, New York, pp 399–468

Chapple WD (1966) Sensory modalities and receptive fields in the abdominal nervous system of the hermit crab, *Pagurus granosimanus* (Stimpson). J Exp Biol 44:209–223

Chapple WD (1977a) Diversity of muscle fibers in the abdominal dorsal superficial muscles of the hermit crab, *Pagurus pollicarus*. J Comp Physiol 121:395–412

Chapple WD (1977b) Motoneurons innervating the dorsal superficial muscles of the hermit crab, *Pagurus pollicarus*, and their reflex asymmetry. J Comp Physiol 121:413–431

Chapple WD (1993) Dynamics of reflex cocontraction in hermit crab abdomen: experiments and a systems model. J Neurophysiol 69:1904–1917

Chapple WD (1997) Regulation of muscle stiffness during periodic length changes in the isolated abdomen of the hermit crab. J Neurophysiol 78:1491–1503

Davis WJ (1969) Reflex organization in the swimmeret system of the lobster. I. Intrasegmental reflexes. J Exp Biol 51:547–563

DiCaprio RA, Clarac F (1983) Reversal of an intersegmental reflex elicited by a muscle receptor organ. J Exp Biol 103:303–306

Dorsett DA (1976) The structure and function of prioprioceptors in soft-bodied invertebrates. In: Mill PJ (ed) Structure and function of prioprioceptors in the invertebrates. Chapman and Hall, London, pp 443–483

Duysens J, Clarac F, Cruse H (2000) Load-regulating mechanisms in gain and posture: comparative aspects. Physiol Rev 80: 83–133

Gnatzy W, Schmidt M, Römbke J (1984) Are the funnel-canal organs the "campaniform sensilla" of the shore crab *Carcinus meanas* (Crustacea, Decapoda)? I. Topography, external structure and basic organization. Zoomorphology 104:11–20

Hiebert GW, Whelan PJ, Prochazka A, Pearson KG (1996) Contribution of hind limb flexor muscle afferents to the timing of phase transitions in the cat step cycle. J Neurophysiol 75: 1126–1137

Horak FB, MacPherson JM (1996) Postural orientation and equilibrium. In: Rowell LB, Shepherd JT (eds) Handbook of physiology. Oxford University Press, Oxford, UK, pp 255–292

Libersat F, Clarac F, Zill S (1987) Force-sensitive mechanoreceptors of the dactyl of the crab: single-unit responses during walking and evaluation of function. J Neurophysiol 57: 1618–1637

Pabst H, Kennedy D (1967) Cutaneous mechanoreceptors influencing motor output in the crayfish abdomen. Z Vergl Physiol 57:190–208

Pearson KG, Collins DF (1993) Reversal of the influence of group Ib afferents from plantaris on activity in medial gastrocnemius muscle during locomotor activity. J Neurophysiol 70:1009–1017

Pflüger HJ, Field LH (1999) A locust chordotonal organ coding for proprioceptive and acoustic stimuli. J Comp Physiol 184: 169–183

Presnell JK, Schreibman MP (1997) Humason's animal tissue techniques. Johns Hopkins University Press, Baltimore

Richmond BJ, Optican LM, Podell M, Spitzer H (1987) Temporal encoding of two-dimensional patterns by single units in primate inferior temporal cortex. I. Response characteristics. J Neurophysiol 57:132–146

Shelton RG, Laverack MS (1968) Observations on a redescribed crustacean cuticular sense organ. Comp Biochem Physiol 25:1049–1059

Silverman BW (1986) Density estimation for statistics and data analysis. Chapman and Hall, London

Sutherland RM, Nunnemacher RF (1968) Microanatomy of crayfish thoracic cord and roots. J Comp Neurol 132:499–518

Torkkeli PH, French AS (2002) Simulation of different firing patterns in paired spider mechanoreceptor neurons: the role of Na^+ channel inactivation. J Neurophysiol 87:1363–1368

Wiersma CAG, Bush BMH (1963) Functional neuronal connections between the thoracic and abdominal cords of the crayfish, *Procambarus clarkii* (Girard). J Comp Neurol 121:207–235

Wiersma CAG, Hughes GM (1961) On the functional anatomy of neuronal units in the abdominal cord of the crayfish, *Procambarus clarkii* (Girard). J Comp Neurol 116:209–228

Zill SN, Moran DT (1981) The exoskeleton and insect proprioception. I. Responses of tibial campaniform sensilla to external and muscle-generated forces in the American cockroach, *Periplaneta americana*. J Exp Biol 91:1–24